RESEARCHERID
THOMSON REUTERS

ISSN: 2277-9655
[Kimunguyi * *et al.*, 6(12): December, 2017] Impact Factor: 4.116
IC™ Value: 3.00 CODEN: IJESS7

IJESRT

INTERNATIONAL JOURNAL OF ENGINEERING SCIENCES & RESEARCH TECHNOLOGY

A NUMERICAL INVESTIGATION OF TURBULENT NATURAL CONVECTION IN A 3-D ENCLOSURE USING FINITE VOLUME METHOD AND STAGGERED GRID

Kimunguyi Kiliswa Josephs[*1], Grace Wambui Gachigua[2] & Francis Kimani Gatheri[3]
[*1]Shekinah P. C. Kiserian, P.O. Box 444 – 00206, Kiserian, Kenya
[2&3]School of Mathematics and Actuarial Science, Technical University of Kenya

DOI: 10.5281/zenodo.1116596

ABSTRACT

The objective of this study is to conduct a numerical investigation of turbulent natural convection in a 3-D cavity using Finite Volume Method and Staggered Grid. The statistical-averaging process of the mass, momentum and energy governing equations introduces unknown turbulent correlations into the mean flow equations which represent the turbulent transport of momentum, heat and mass, namely Reynolds stress $(\overline{u_\iota u_j})$ and heat flux $(\overline{u_\iota \theta})$, which are modelled using k-ω SST model. The Reynolds-Averaged Navier-stokes (RANS), energy and k-ω SST turbulent equations are first non-dimensionalized and the resulting equations are discretized using Finite Volume Method. The results showed an efficient and cost effective procedure for solving a turbulent natural convection problem was by use of an optimized staggered grid and the flow domain discretized by use of Finite Volume Method

KEYWORDS: Turbulence natural Convention, Staggered grid, k-ω SST, Finite Volume method.

I. INTRODUCTION

In fluid dynamics, turbulence is a flow regime characterized by chaotic and stochastic changes. This includes low momentum diffusion, high momentum convection and rapid variation of pressure and velocity in space and time. Finite Volume Method is among the most powerful means of solving different engineering problems in fluid dynamics. The physical domain is divided by cells to form a numerical mesh, which can be unstructured in turbulence modelling. The flow field variables are evaluated in some discrete points on each cell and are interpreted as average value over the finite volumes. The conservation laws are then applied to the finite volumes to obtain the discrete equations.

II. MATHEMATICAL FORMULATION

In this thesis, a numerical investigation of turbulent natural convection within a 3-D is conducted using the staggered grid and the finite volume method. The geometry is illustrated in figure 3.1. It consists of a hot surface, located on the left side of the rectangular cavity wall, and a cold surface on the right side. The enclosure is heated on the hot wall (Red color) and cooled on the cold wall (blue color). The measurement of Ampofo and Karyiannis (2003) were used. The hot and cold walls of the cavity were isothermal at 323 ± 0.15K and 283 ± 0.15K respectively, giving a Reyleigh number of 1.58×10^9. Each of the remaining walls are adiabatic. All boundaries of the enclosure are stationary, non-slip, rigid and impermeable.

The walls measures 0.75m by 0.75m wide by 1.5m and the following the boundary conditions are applied;

- The choice of the non-dimensional Θ temperature was such that $0 \leq \Theta \leq 1$.
- The Dirchlet boundary conditions apply on the heater and the window, while the Neumann boundary condition applies on the adiabatic walls.
- No slip boundary condition is used at the solid wall boundary of the 3-D enclosure.
- Free slip boundary holds for the component of velocity normal to the impermeable wall surfaces.

The initial pressure correction value p' at the rigid and stationary wall boundary is zero. Initially, the fluid is motionless the temperature of which is equal to the average temperature of the vertical walls.

ISSN: 2277-9655
Impact Factor: 4.116
CODEN: IJESS7

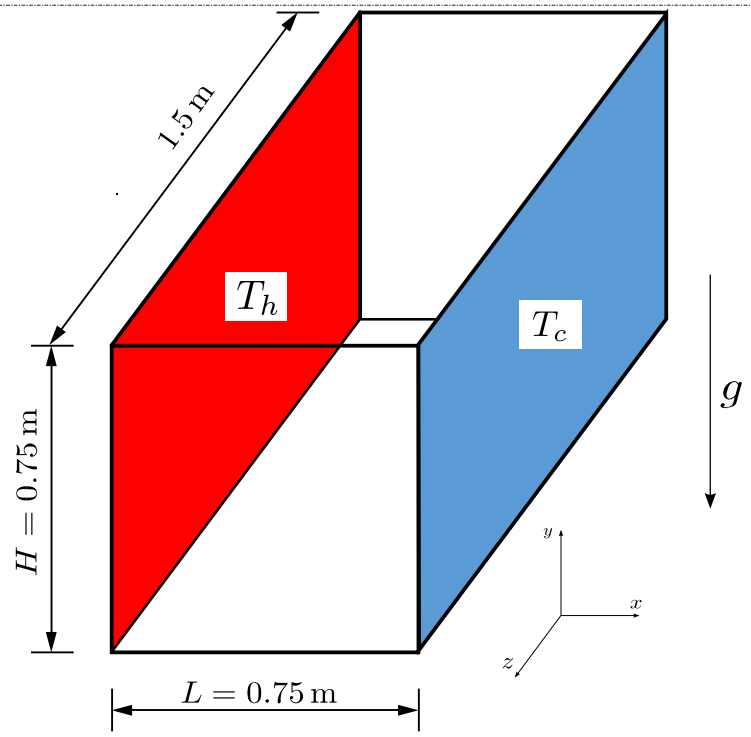

Fig. 2.1 Geometry of the 3-D numerical model

The fluid to be used is air. Therefore fluid flow will depend only on the temperature difference given as $\Delta T = T_h - T_w$. Aspect ratio A=H/L=0.5, Where H is the height and L is the Length of the enclosure. The characteristic length is taken to be the size of the enclosure in the $x-$ direction. Furthermore, the Boussinesq Approximation (1903) is assumed and is presented below.

The cell distribution within the flow domain is optimized, whereby the cells are made finer in areas where large variations or gradients occur from point to point and coarser in regions with relatively small variations in the solved variables.

III. GOVERNING EQUATIONS

The equations governing the flow of incompressible Newtonian fluid are derived from equations, which enforce the conservation of mass, the conservation of momentum, and conservation of energy. The equation of continuity, the momentum equation and the energy equation are given as equations (3.1), (3.2) and (3.3) below respectively:

$$\frac{\partial \rho}{\partial t} + \frac{\partial}{\partial x_j}(\rho u_j) = 0 \tag{3.1}$$

$$\frac{\partial}{\partial t}\rho u_j + \frac{\partial}{\partial x_j}\rho u_i u_j = -\frac{\partial P}{\partial x_i} + \rho g_i + \frac{\partial}{\partial x_j}\left[\mu\left(\frac{\partial u_i}{\partial x_j} + \frac{\partial u_j}{\partial x_i}\right) + \mu_s \delta_{ij}\frac{\partial u_k}{\partial x_k}\right] \tag{3.2}$$

Where μ and μ_s are the first and second coefficient of viscosity.

$$\frac{\partial}{\partial t}(C_P \rho T) + \frac{\partial}{\partial x_j}(C_P \rho u_j T) = \frac{\partial}{\partial x_j}\left(\lambda \frac{\partial T}{\partial x_j}\right) + \beta T\left(\frac{\partial p}{\partial t} + \frac{\partial u_j p}{\partial x_j}\right) + \Phi \tag{3.3}$$

IV. TURBULENCE MODELING

Reynolds Decomposition

The concept entails decomposing the instantaneous fluid flow quantities (variables) in the Navier-Stokes equations into mean (time-averaged) value and fluctuating value.

Instantaneous Equations of Motion

ISSN: 2277-9655
Impact Factor: 4.116
CODEN: IJESS7

A turbulent flow instantaneously satisfies the Navier-Stokes equations and the equations of motion for the instantaneous variables are;

$$\frac{\partial \tilde{\rho}}{\partial t} + \frac{\partial}{\partial x_i}\left(\tilde{\rho}\tilde{u}_j\right) = 0 \tag{4.1}$$

$$\frac{\partial}{\partial t}\tilde{\rho}\tilde{u}_j + \frac{\partial}{\partial x_j}\tilde{\rho}\tilde{u}_i\tilde{u}_j = -\frac{\partial \tilde{P}}{\partial x_i} + \tilde{\rho}g_i + \frac{\partial}{\partial x_j}\left[\mu\left(\frac{\partial \tilde{u}_i}{\partial x_j} + \frac{\partial \tilde{u}_j}{\partial x_i}\right) + \mu_s\delta_{ij}\rho\frac{\partial \tilde{u}_k}{\partial x_k}\right] \tag{4.2}$$

$$\frac{\partial}{\partial t}\left(\tilde{C}_P\tilde{\rho}\tilde{T}\right) + \frac{\partial}{\partial x_j}\left(\tilde{C}_P\tilde{\rho}\tilde{U}_j\tilde{T}\right) = \frac{\partial}{\partial x_j}\left(\lambda\frac{\partial \tilde{T}}{\partial x_j}\right) + \beta T\left(\frac{\partial \tilde{p}}{\partial t} + \frac{\partial \tilde{u}_j\tilde{p}}{\partial x_j}\right) + \Phi \tag{4.3}$$

The equations satisfied by the mean flow are obtained by substituting the Reynolds decomposition into the instantaneous Navier-Stokes equations and taking the average of the equations

Averaged Equations of Motion

a) Continuity equation for Turbulent flow

Decomposing the instantaneous differential form of the continuity equation (4.2) into its mean and turbulent part, taking the time average and simplifying yields;

$$\frac{\partial \bar{\rho}}{\partial t} + \frac{\partial}{\partial x_j}\left(\bar{\rho}\bar{u}_j + \overline{\rho' u_j'}\right) = 0 \tag{4.4}$$

b) Momentum Equation for Turbulent Flow

Decomposing the instantaneous dependent variables of the momentum equation, taking the average, expanding and then simplifying this equation yields:-

$$\overline{\frac{\partial}{\partial x_j}\left[\mu\left(\frac{\partial(\bar{u}_\iota + u_\iota')}{\partial x_j} + \frac{(\bar{u}_j + u_j')}{\partial x_\iota}\right) + \mu_s\delta_{\iota\jmath}\rho\frac{\partial(\bar{u}_k + u_k')}{\partial x_k}\right]} = \frac{\partial}{\partial x_j}\left[\mu\left(\frac{\partial \bar{u}_i}{\partial x_j} + \frac{\partial \bar{u}_j}{\partial x_i}\right) + \mu_s\delta_{ij}\frac{\partial \bar{u}_k}{\partial x_k}\right] \tag{4.5}$$

The correlation $\overline{u_\iota u_\jmath}$ in equation (4.5) is generally nonzero.

(a) Mean Heat Equation

Decomposing the instantaneous temperature variable in the heat equation into the mean part and the deviation from the mean, and simplifying this equation yields;

$$\frac{\partial}{\partial t}\left(C_P\bar{\rho}\bar{T} + C_P\overline{\rho' T'}\right) + \frac{\partial}{\partial x_j}\left(C_P\overline{\rho u_j}\bar{T}\right) = \frac{\partial \bar{p}}{\partial t} + \frac{\partial \bar{p}}{\partial x_j} + \overline{u'_\iota\frac{\partial p'}{\partial x_j}} + \frac{\partial}{\partial x_j}\left(\lambda\frac{\partial \bar{T}}{\partial x_j} - C_P\bar{\rho}\overline{u'_\iota T'} - C_P\overline{\rho' u_\iota T'}\right) + \bar{\Phi} \tag{4.6}$$

Where;

$$\bar{\Phi} = \overline{\tau_{\iota\jmath}}\frac{\partial \bar{u}_\iota}{\partial x_j} + \overline{\tau'_{\iota\jmath}\frac{\partial u'_\iota}{\partial x_j}} \tag{4.7}$$

V. NON-DIMENSIONALISATION

This implies the partial or full removal of units from an equation involving physical quantities by a suitable substitution of variables. This technique can simplify and parametize problems where measured units are involved. Hence equations (4.4), (4.5), (4.6) and the two $k-\omega$ *SST* model equations take the form

$$\frac{\partial \rho}{\partial t} + \frac{\partial}{\partial x_j}\left(\rho U_i + \overline{\rho u_j}\right) \tag{5.1}$$

ISSN: 2277-9655
Impact Factor: 4.116
CODEN: IJESS7

$$\frac{\partial}{\partial t}(\rho U_i + \overline{\rho u_\iota}) + \frac{\partial}{\partial x_j}\left(\rho U_i U_j + U_i\overline{\rho u_j}\right) = -N_1\frac{\partial P}{\partial x_i} + N_2 p g_i + \frac{\partial}{\partial x_j}\left(N_3\tau_{ij} - U_i\overline{\rho u_\iota} - \rho\overline{u_\iota u_j} - \overline{\rho u_\iota u_j}\right) = 0 \qquad (5.2)$$

$$\frac{\partial}{\partial t}(c_P\rho\Theta + c_P\overline{\rho\Theta}) + \frac{\partial}{\partial x_j}\left(c_P\overline{\rho U_j\Theta}\right) = L_1\left[\frac{\partial p}{\partial t} + U_j\frac{\partial p}{\partial x_j} + \overline{u_j\frac{\partial p}{\partial x_j}}\right] + \frac{\partial}{\partial x_j}\left(L_2\lambda\frac{\partial\Theta}{\partial x_j} - c_P\overline{\rho\Theta} + c_P\rho\Theta\right) + L_3\emptyset \qquad (5.3)$$

$$\frac{\partial}{\partial t}\rho k + \frac{\partial}{\partial x_j}(\rho U_i k) = A_1\overline{u_j\frac{\partial\mu}{\partial x_j}}\left(\frac{\partial u_i}{\partial x_j} + \frac{\partial u_j}{\partial x_i}\right) - \frac{1}{2}\frac{\partial}{\partial x_j}\overline{\rho u_\iota u_j}\frac{\partial U_i}{\partial U_j} + B_2\overline{\rho u_\iota}g_i - B_3\overline{u_j\frac{\partial p}{\partial x_\iota}} \qquad (5.4)$$

$$\frac{\partial}{\partial t}\rho\omega + \frac{\partial}{\partial x_j}\left(\rho U_j\omega\right) = -\frac{\partial}{\partial x_k}\left(B_1\overline{\mu u_k\frac{\partial u_\iota}{\partial x_j}\frac{\partial u_\iota}{\partial x_j}} + 2B_2\nu\frac{\partial u_k}{\partial x_i}\frac{\partial u_\rho}{\partial x_i} - B_1\mu\frac{\partial\omega}{\partial x_k}\right) - 2B_1\mu\frac{\partial U_i}{\partial x_j}\left(\frac{\partial u_i}{\partial x_j}\frac{\partial u_k}{\partial x_j} + \frac{\partial u_j}{\partial x_j}\frac{\partial u_j}{\partial x_k}\right) - 2B_1\mu\frac{\partial^2 U_i}{\partial x_j\partial x_k}\overline{\mu_k\frac{\partial u_\iota}{\partial x_j}} \qquad (5.5)$$

VI. METHOD OF SOLUTION

Introduction

After the conservation laws governing heat transfer, fluid flow and other related processes are expressed in differential form and modeled inform of temperature and velocity, they can be solved using numerical methods, rather than analytical methods, to determine pressure, temperature, mass flux, etc. for various situations and boundary conditions.

Discretization of the Solution Domain using FVM

The process of space discretization involves dividing the computational domain into a finite number of contagious control volumes, where the resulting statements express the exact conservation of relevant properties for each control volumes. At the centroid of each control volumes, the variable values are calculated. Interpolation is used to express variable values at the control volume surface in terms of the center values and suitable quadrature formulae are applied to approximate the surface and volume integrals.

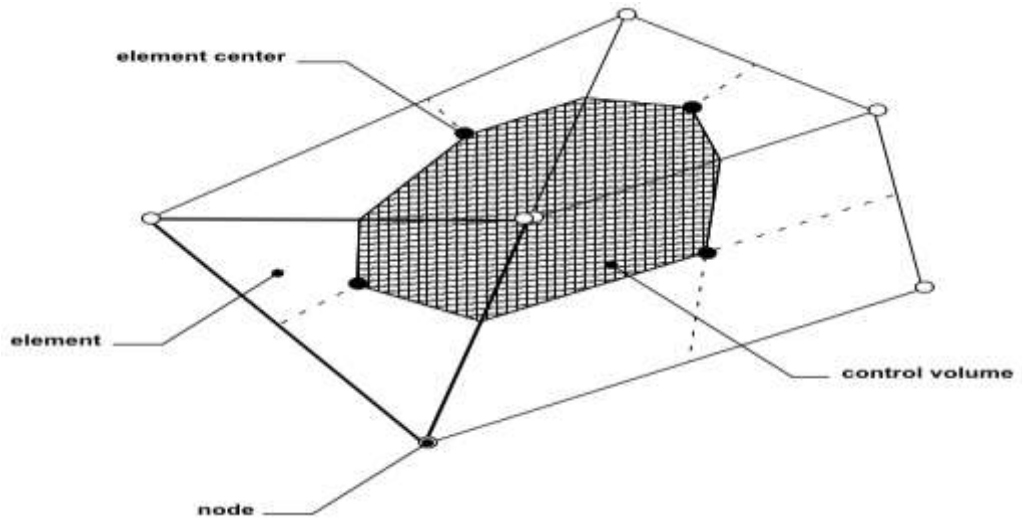

Fig. 6.1 Control-volume element

Figure 6.1, above shows a typical two-dimensional mesh. Finite Volume Method was preferred to Finite Difference Method for the following reasons:

i) Spatial discretization is totally flexible. This type of unstructured mesh offers greater flexibility in order to accommodate irregularly shaped boundaries. Hence you can handle complex geometries, reduce geometric errors and give more resolutions in regions of interest

ii) FVM naturally conserves variables when applied to PDEs expressing conservation laws since, as two neighboring cells share a common interface, the total flow of a conserved quantity out of one cell will be the same as that entering the other cell. As a result, mass, momentum and energy are conserved even on coarse grids.

iii) This method requires no transformation of equations in terms of body-fitted coordinate system as is required in Finite-Difference Method.

iv) FVM enjoys an advantage in memory use and speed for higher speed flows and turbulent flows.

Variable Arrangement on the Grid

Before describing the discretization scheme, choice of arrangement on the grid requires some consideration. Instead of a collocated grid, we used a staggered grid arrangement for this thesis computation in order to evaluate the velocity components at the control volume faces while the rest of the variables governing the flow field, such as the pressure, temperature, and turbulent quantities, are stored at the central node of the control volumes. A typical arrangement is depicted in figure 6.2, which is in 2-D, for convenience.

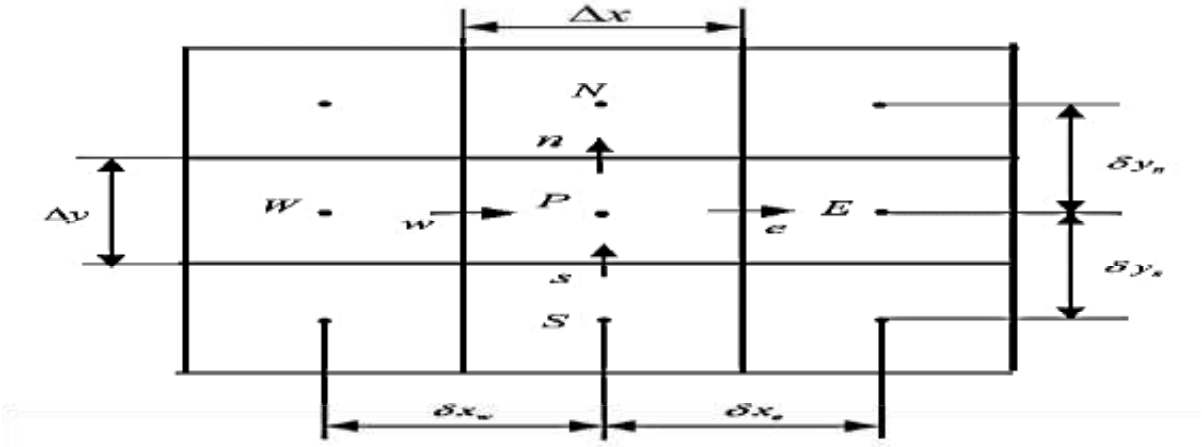

Fig. 6.2 control volumes in 2D.

It can be demonstrated that the discrete values of the velocity components, u, from the $x-$momentum equation are evaluated and stored at the east, e, and the west, w, faces of the control volume. By evaluating the other velocity components using the $y-$momentum and $z-$momentum equations on the rest of the control volume faces, these velocities allow a straightforward evaluation of the mass fluxes that are used in the pressure correction equation. This arrangement therefore provides a strong coupling between the velocities and pressure, which helps to avoid some types of convergence problems and oscillations in the pressure and velocity fields.

Discretization of the Governing Equations Using FVM

The process of discretization of the governing equations involved developing a set of algebraic equations (based on discrete points in the flow domain) to be used in the place of the partial differential equations.

An algebraic equation for each of the control volumes can be obtained, in which a number of the neighboring nodal values appear.

Discretization of the Continuity Equation by FVM

Consider the continuity equation (3.1) in two dimensional form of figure 6.2. Integrating over the cell P and applying Gauss' divergence theorem to the volume integral, we get;

$$\frac{1}{\Delta V}\int_V \nabla . UdV = \frac{1}{\Delta V}\int_A UdA \qquad (6.1)$$

ISSN: 2277-9655
Impact Factor: 4.116
CODEN: IJESS7

Assuming that the velocity variable on the face is represented by its centroid value, we may write;

$$\frac{1}{\Delta V}\int_A UdA = \frac{1}{\Delta V}\sum_i U_i A_i \tag{6.2}$$

For a first-order derivative of U in two dimensions, the term along the x direction represented in equation (3.1), can be approximated by;

$$\left(\frac{\partial u}{\partial x}\right) = \frac{1}{\Delta V}\int_V \frac{\partial u}{\partial x}dV = \frac{1}{\Delta V}\int_A udA^x \approx \frac{1}{\Delta V}\sum_{i=1}^{N} u_i A_i^x \tag{6.3}$$

Where u_i the velocity variable values at the elemental surfaces and N denotes the number of bounding surfaces on the elemental volume. For a quadrilateral element in 2-D for the structured mesh as seen in figure 6.2, N has the value of four since there are four bounding surfaces of the element. In 3-D, for a hexagonal element, N becomes six. Similarly, the first-order derivative for U in the y direction is obtained in the same fashion, which can be written as;

$$\left(\frac{\partial v}{\partial y}\right) = \frac{1}{\Delta V}\int_{\Delta V} \frac{\partial v}{\partial y}dV = \frac{1}{\Delta V}\int_A vdA^y \approx \frac{1}{\Delta V}\sum_{i=1}^{N} v_i A_i^y \tag{6.4}$$

It follows from equation (6.2) that the first order derivative for U in the z direction can be written as;

$$\left(\frac{\partial w}{\partial y}\right) = \frac{1}{\Delta V}\int_{\Delta V} \frac{\partial w}{\partial y}dV = \frac{1}{\Delta V}\int_A wdA^z \approx \frac{1}{\Delta V}\sum_{i=1}^{N} w_i A_i^z \tag{6.5}$$

For our considered mesh (orthogonal) in figure 6.2, using equations (6.2), (6.3) and (6.4), we get;

$$(u_e - u_w)\Delta y + (v_n - v_s)\Delta x = 0 \tag{6.6}$$

In 3-D, equation (6.6) becomes;

$$[(\rho u)_e - (\rho u)_w]\Delta y\Delta z + [(\rho v)_n - (\rho v)_s]\Delta z\Delta x + [(\rho w)_t - (\rho w)_b]\Delta x\Delta y = 0 \tag{6.7}$$

Discretization of the Momentum Equation by FVM

Consider the 2-D rectangular domain shown in figure 6.2. Assume that;

(i) the velocity vector U and the pressure P are stored at the cell centroids
(ii) a steady state

The momentum equation in equation (3.2) in x and y may be written as;

$$\nabla.(\rho V u) = \nabla.(\mu\nabla u) - \nabla P.i + S_u \tag{6.8}$$
$$\nabla.(\rho V v) = \nabla.(\mu\nabla u) - \nabla P.i + S_v \tag{6.9}$$

Each of the momentum equations contains a pressure gradient term, a source term (S_u and S_v) which contains the force term, as well as remnants of the stress tensor term.

ISSN: 2277-9655
Impact Factor: 4.116
CODEN: IJESS7

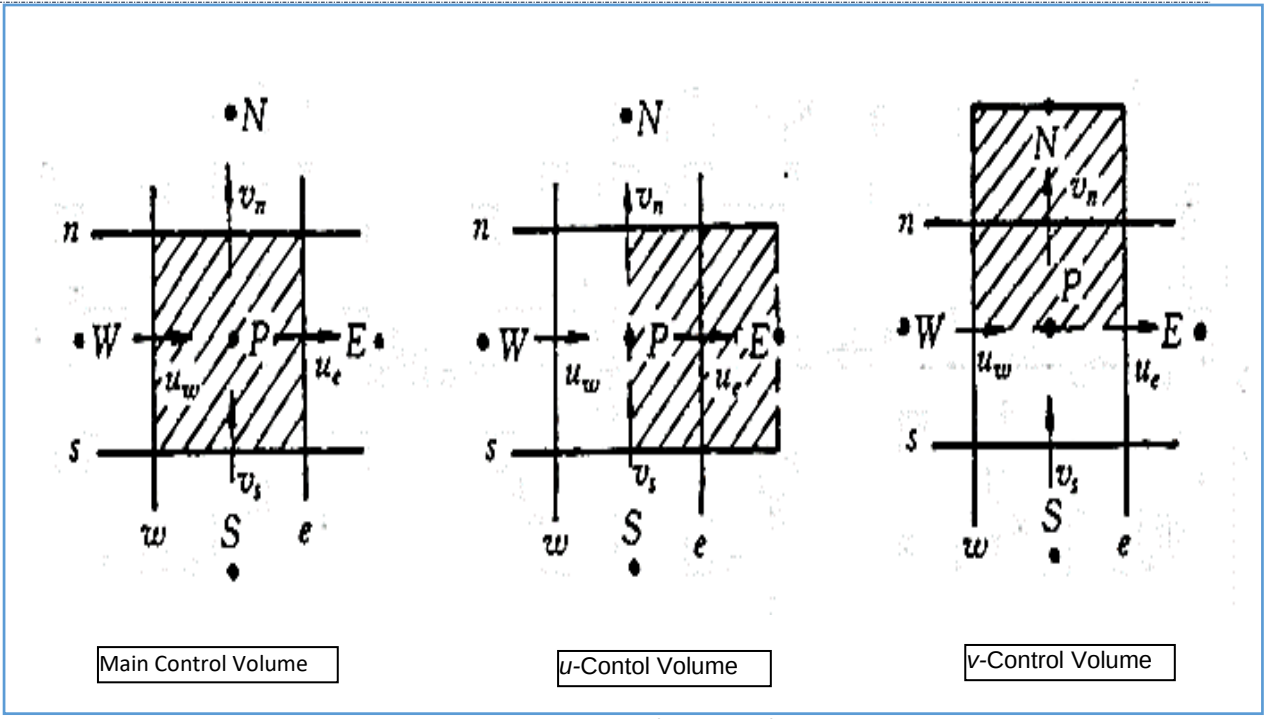

Fig. 6.3 The Staggered Grid $\frac{\partial p}{\partial x} = \frac{P_E - P_P}{(\partial x)_e} \frac{\partial p}{\partial y} = \frac{P_N - P_P}{(\partial y)_n}$

Using the staggered grid for the velocity components as in figure 6.3, as used by Harlow and Welch (1965) in their MAC method, the resulting discretized momentum equation, in the x −direction, can be written;

$$a_e u_e = \sum a_{nb} u_{nb} + b + (P_P - P_E) A_e \qquad (6.10)$$

where a_e is the coefficient for the main grid point, a_{nb} are the neighbor coefficients that account for the combined convection-diffusion at the control-volume faces. Here P is the main grid point. The staggering is in the x direction only, such that the faces normal to that direction pass through the main grid points P and E, $b = S_c \Delta x \Delta y + a_P^o \emptyset_P^o$ in which S_c is the source term quantity; The term $(P_P - P_E)A_e$ is the pressure force acting on the u control volume, A_e being the area which the pressure difference acts. For three-dimensional case, A_e will stand for $\Delta y \Delta z$.

The momentum equation for the y −direction momentum equation is staggered in the y −direction. Hence the discretization equation for v_n is given as;

$$a_n v_n = \sum a_{nb} v_{nb} + b + (P_P - P_N) A_n \qquad (6.11)$$

Similarly, the z −direction momentum equation is staggered in the z −direction and given as;

$$a_n w_t = \sum a_{nb} w_{nb} + b + (P_P - P_t) A_t \qquad (6.12)$$

Where;
$(P_P - P_t)A_t$ is the pressure force acting on the w control volume, where A_t is the area which the pressure difference acts.

The momentum equations (6.10), (6.11) and (6.12) can be solved using the following discretized velocity and pressure correction equations, after making an initial guess for the pressure field;

$$u_e = u_e^* + d_e(p_P' - p_E') \qquad (6.13)$$
$$v_n = v_n^* + d_n(p_P' - p_N') \qquad (6.14)$$
$$w_t = w_t^* + d_t(p_P' - p_T') \qquad (6.15)$$
$$a_P p_P' = a_E p_E' + a_W p_W' + a_N p_N' + a_S p_S' + a_T p_T' + a_B p_B' + b \qquad (6.16)$$

Where u^*, v^* and $w^*$are imperfect velocity fields based on the guessed pressure field p^* and u', v', w', $p'$are velocity and pressure correction factors.

ISSN: 2277-9655
Impact Factor: 4.116
CODEN: IJESS7

$$d_e = d_n = d_t \equiv \frac{A_e}{a_e} \tag{6.17}$$

Where;

$$\left.\begin{aligned} a_E &= \rho_e d_e \Delta y \Delta z \\ a_W &= \rho_w d_w \Delta y \Delta z \\ a_N &= \rho_n d_n \Delta z \Delta x \\ a_S &= \rho_s d_s \Delta z \Delta x \\ a_T &= \rho_t d_t \Delta x \Delta y \\ a_B &= \rho_b d_b \Delta x \Delta y \\ a_P &= a_E + a_w + a_N + a_S + a_T + a_S \end{aligned}\right\} \tag{6.18}$$

$$b = \frac{(\rho_P^0 - \rho_P)\Delta x \Delta y \Delta z}{\Delta t} + [(\rho u^*)_w - (\rho u^*)_e]\Delta y \Delta z + [(\rho v^*)_s - (\rho v^*)_n]\Delta z \Delta x + [(\rho w^*)_b - (\rho w)_t]\Delta x \Delta y$$

We have hence formulated all the equations needed for obtaining the velocity components and pressure. The application of SIMPLEC algorithm, to solve equations (6.13), (6.14), (6.15) and (6.16) is discussed in section (6.6).

VII. RESULTS AND DISCUSSION

The results presented here were obtained by solving equations (6.13), (6.14), (6.15) and (6.16) numerically using the staggered grid and finite volume method; and together with the boundary conditions given at section (2). The numerical results we have found were, validated against the benchmark data provided Sanjurjo and Cooper (1991) and by Ampofo) and Karayiannis (2003), at a Rayleigh number of 1.58×10^9.

Grid Convergence

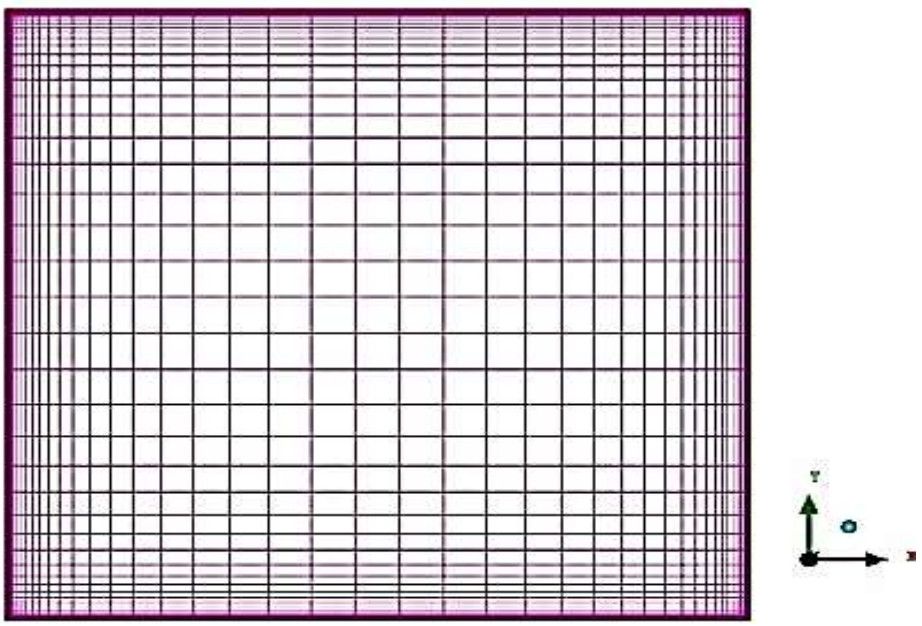

Fig 7.1 grid 80x80

The grid shown in figure 7.1 above is the standard grid used in these validations. The computational grids are staggered and clustered towards the walls. Grids are staggered so that the scalar variables like pressure, temperature, density and turbulent quantities are stored in the cell centres of the control volume whereas vector

ISSN: 2277-9655
Impact Factor: 4.116
CODEN: IJESS7

variables like velocity and momentum are located in the cell faces. This would provide a strong coupling between velocities and pressure. Hence the odd-even decoupling, a discretization error that would lead to checker-board patterns in the solution, leading to convergence issues is sorted out. Grids are clustered towards the wall because, the flow in turbulent natural convection in an enclosure is characterized by a thin boundary layer along the walls while the core is thermally stratified. The flow gradient are very large in the boundary layer and require a large number of computational grids, in which the values of dependent variables should be determined in order to capture the flow physics, hence the adaptive refinement towards the isothermal walls which is our region of interest. All variables are calculated right up to the walls without using any wall function since the $k-\omega\ SST$ model would use its blending function to switch the model to the $k-\omega$ model which is more accurate and more numerically stable in the near wall regions. On the wall surface, the boundary values for the velocity components and the turbulent kinetic energy are set to zero in conformity with no slip boundary condition.

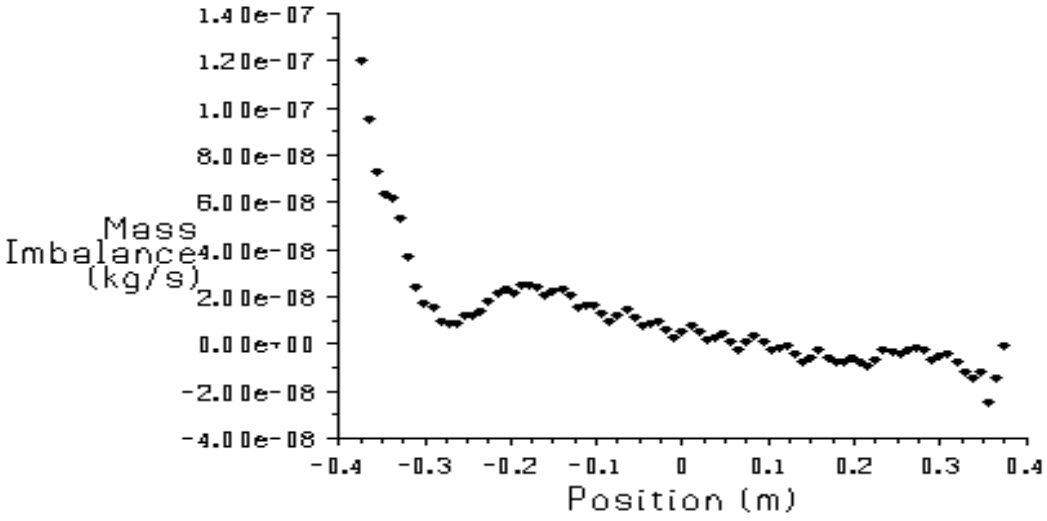

Fig 7.2 Mass imbalance profiles on an 80x80 grid

The dimensionless temperature of the cold and hot walls are 0 and 1 respectively.
For a numerical method to bear a stable discretization equation solution / a grid independent solution;

i) The solved variables at all discrete cell locations should not change significantly with further grid refinement/ as the grid density increases.
ii) The computational domain should be devoid of distorted cells (long thin cells) because grid cell distortion leads to a poorly converged solution.

This outlines the importance of carrying out a mesh convergence test using a grid checker. This we did by carrying out a grid independence test. This was done by computing the numerical solution on successively finer grids. The difference in numerical solution between the coarse (80x80) and finer (160x160) grid, was to be taken as the accuracy measure of the coarse grid.

In this case, the 80x80 grid was refined by increasing the number of grid points to 160x160 for confirmation of grid independence. Figures 7.1 and 7.2 show a comparison of the residual mass imbalance profiles for the flow generated on each of the grids. The numerical implication is that as the mesh spacing or control volume size approached zero, the discretized equation solution matches the exact solution.

Initially we did a test run using a coarse mesh. This had the following advantages

i) It gave us the opportunity to evaluate the computers storage and running time.
ii) By this way, it was possible to assess the convergence and divergence behavior of the solutions

ISSN: 2277-9655
Impact Factor: 4.116
CODEN: IJESS7

iii) The test run provided us with means of rectifying possible sources of solution errors such as physical modelling or human errors.

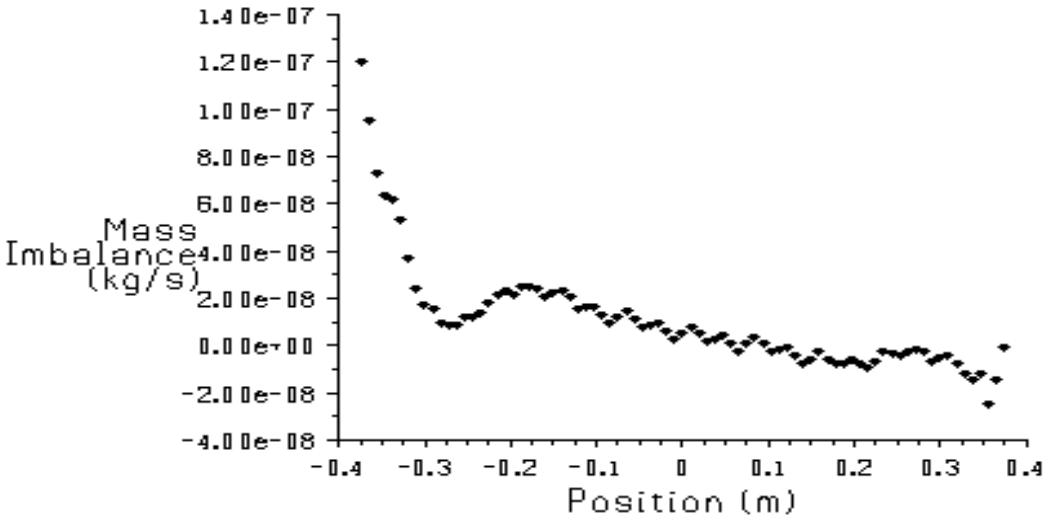

Fig 7.3 Mass imbalance grid on a 160x160 grid

Evidently, the results obtained on the 80x80 grid do not differ from those obtained on the 160x160 grid layout. Therefore, we can conclude the discretization error has diminished to zero and the grid independence has been reached.

Through the grid independence test we established that;

i. The discretization equation results do not depend on profile assumption.
ii. We have reduced computational cost by finding an optimum grid size of the control volume, without compromising with the accuracy of the solution

VIII. CONCLUSION

i) From the numerical data, the numerical method produced a solution which approached the exact solution by Ampofo and Karayiannis (2003) as the grid spacing reduced to zero. Further, the method is stable and consistent as evidenced by the damping errors as the numerical method proceeded and the similarity of this flow to that observed in the experimental results by Sanjurjo and Cooper (1991). Therefore using Lax's equivalence theorem, Lax and Richtmyer (1956), this code is valid, stable and consistent.

ISSN: 2277-9655
Impact Factor: 4.116
CODEN: IJESS7

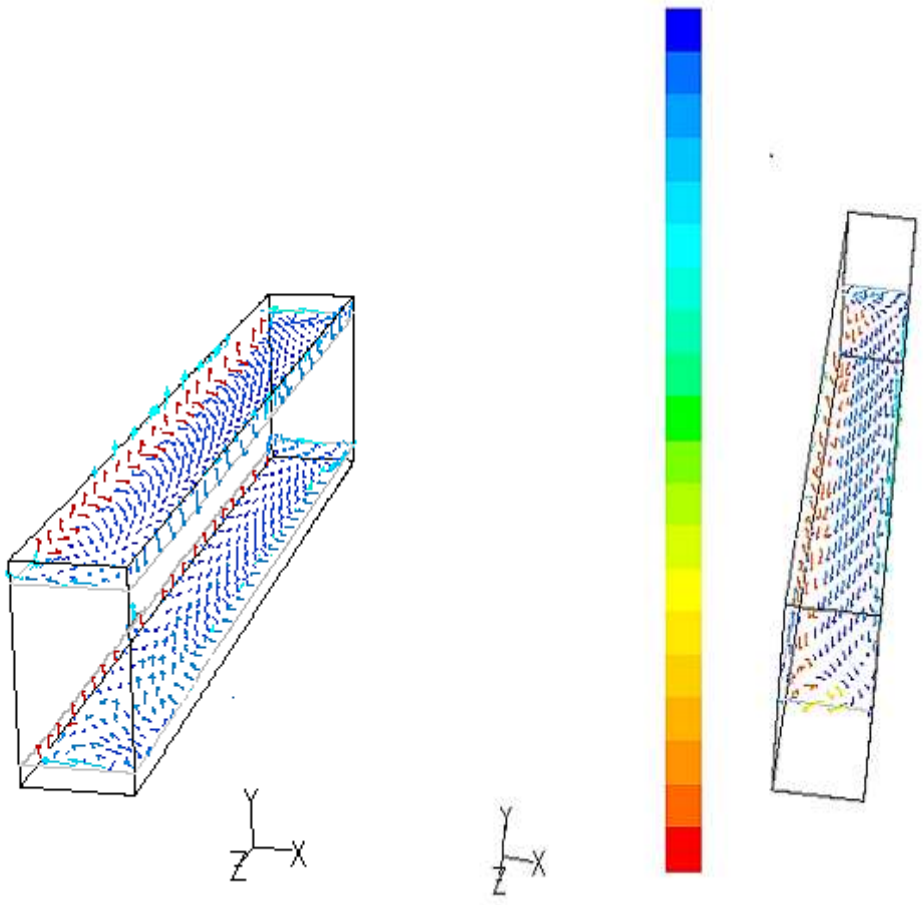

Fig 8 (a) Velocity vectors at Y=0.1 and Y=0.9 (b) Velocity vectors at Y=0.5

ii) In this paper, an efficient procedure for solving a turbulent natural convection problem has been developed by use of an optimized staggered grid and the flow domain is discretized by use of Finite Volume Method. Its efficiency is illustrated by applying it to the problem of turbulent natural convection in an enclosure, heated on the hot wall and cooled on the cold wall.

iii) By use of the Finite Volume Method, the flow domain was properly discretized with an appropriate grid distribution. The accuracy of a solution and its associated cost due to computing time and hardware were dependent in part on the grid density. Some cost savings was achieved by optimizing and staggering the grid.

IX. ACKNOWLEDGEMENT

My sincere gratitude to Prof. F. K. Gatheri and Dr. G. W. Gachigua for their contribution, support and inspiration

REFERENCES

[1] **Ampofo F. and Karanyiannis T. G. (2003)**, Experimental Benchmark Data for Turbulent Natural Convection in an Air-Filled Square Cavity, *Intenational Journal of Heat Mass Transfer*, **46**, 3551-3572

[2] **Berghein C., Penot F., Mergui S. and Allard F. (1993)**, Numerical and experimental evaluation of turbulent models for natural convection simulation in a thermally driven square cavity, *Proceedings on Adaptive Selection Mode Error Concealment (ASMEC) Conference*, 1-12.

[3] **Boussinesq J. (1903)**, *Th´eorie Analytique de la Chaleur, Gauthier-Villars*, **2**, 1-680

[4] **Davidson L. and Nielsen P.V. (1996)**, Large Eddy Simulations of the Flow in a Three- Dimensional Ventilated Room, *Proceedings Roomvent '96*, **2**, 161-168.

ISSN: 2277-9655
Impact Factor: 4.116
CODEN: IJESS7

[5] **Dol H. S. and Hinjalic K.** (2001), Computational Study of Turbulent Natural Convention in a side Heated Near-cubic Enclosure at High Re, *International Journal of Heat and Mass Transfer*, **4**, 2323-2344

[6] **Gatheri F. K. (2005)**, Variable False Transient for the Solution of Coupled Elliptic Equations, East African Journal of Physical Sciences, **6** (2), 117

[7] **Gatheri F. K., Reizes J., Leonardi E. and Graham del Vahl Davis (1993)**, The use of Variable False Transient Factors for the Solution of Natural Convection Problems, *Australian Heat and Mass Transfer*, University of Queensland, **5**, 68

[8] **Gatheri F. K., Reizes J., Leonardi E., and Graham del Vahl Davis (1994)**, Natural Convection in an Enclosure with Localized Heating and Cooling: A numerical Study, Heat Transfer 1994, G.F. Hewitt (ed), **2**, 361-366

[9] **Lax P. D. and Richtmyer R. D. (1956)**, Survey of the Stability of Linear Finite Difference Equations, *Communications on Pure and Applied Mathematics*, **9**, 267-293.

[10] **Pantaker S. V. (1980)**, Numerical Heat Transfer and Fluid Flow, Series in Computational Methods in Mechanics and Thermal Sciences, 1st Edition, Hemisphere Publishing Corporation, 25-39

[11] **Sanjurjo, B. E. and Cooper, P. (1991)**, Experimental investigation of air movement in a room using a water-filled scale model, Australian *Institute of Refrigeration, Air Conditioning and Heating (AIRAH) Conference*, Melbourne, Australia.

[12] **Tian J. and Karayiannis T.G. (2001)**, Low turbulence natural convection in an air filled square cavity, J. Heat and Mass Transfer, **43**, 849-866

[13] **Tian, Y.S. and Karayianins, T.G. (2000)**, Low Turbulence Natural Convection in an Air Filled Square Cavity, Part I: The Thermal and Fluid Flow Fields. *International Journal of Heat and Mass Transfer*, **43**, 849-866

CITE AN ARTICLE

Kimunguyi K. J, Gachigua, G. W., & Gatheri, F. K. (n.d.). A NUMERICAL INVESTIGATION OF TURBULENT NATURAL CONVECTION IN A 3-D ENCLOSURE USING FINITE VOLUME METHOD AND STAGGERED GRID. INTERNATIONAL JOURNAL OF ENGINEERING SCIENCES & RESEARCH TECHNOLOGY, 6(12), 172-183.